Upstream and Downstream Analysis of an Optical Fronthaul System Based on DSP-Assisted Channel Aggregation

Upstream and Downstream Analysis of an Optical Fronthaul System based on DSP-Assisted Channel Aggregation

Pablo Torres-Ferrera, Stefano Straullu, Silvio Abrate and Roberto Gaudino

***Abstract*—In this paper we focus on a well-known optical fronthauling architecture based on frequency division multiplexed DSP-assisted channel aggregation and we present new results related to the optimization of the optical setup, proposing an efficient technique for the optimization of the transmission. In particular, we report an original pre-emphasis technique to equalize the performance of the radio channels, especially focusing on the upstream link that has more critical characteristics but was typically not treated in details in previous works on this topic. The effects of both radio and optical impairments on the error vector magnitude (EVM) are taken into account. An analytical description of our approach is provided, and then it is applied on an experimental setup (able to aggregate up to 96 20 MHz radio signals), showing the possibility of minimizing the maximum EVM at the output of the fronthauling link, for both downstream and upstream transmission. Additionally, a low-complexity technique to practically estimate the EVM per channel by taking advantage of only the DSP-aggregation/de-aggregation functionalities is proposed and, again, experimentally demonstrated.**

***Index Terms*— Mobile Fronthaul, Frequency Division Multiplexing, OFDM, DSP-assisted channel aggregation, Radio-over-Fiber.**

I. Introduction

There is a wide consensus around the fact that high-capacity optical fronthaul technology is becoming imperative in order to fulfill the technical requirements of next generation mobile networks [1–4]. An exceedingly high aggregated bit rate on the optical fronthaul segment would be required if the today de-facto CPRI [5] standard was directly applied to transport a large number of LTE-A or 5G radio signals. A promising alternative based on DSP-assisted channel aggregation (DSP-A), which provides huge bandwidth saving with respect to CPRI, has recently emerged [6]. The key feature of this approach consists on "natively" transporting the radio waveforms over the optical link by using a frequency division multiplexing (FDM) approach. FDM is performed using only low latency and relatively low complexity DSP functionalities, enabled by the use of efficient Fast Fourier transform (FFT) and inverse FFT (iFFT) blocks.

For the sake of clarity, the main principles of DSP-assisted channel aggregation are reported hereafter. The most typical embodiment [6] implements the following functionalities in the downstream (DS) direction:

- an FFT over a small number of N-points on each of the N_{ch} baseband radio waveforms, to be simultaneously transported to the Antenna Site (AS);
- FDM aggregation of the N_{ch} FFT outputs by placing the spectral samples in the proper position of a large M points vector, which is then sent to an M-points inverse FFT to generate the aggregated time domain signal;
- optical transmission of the resulting signal using analog intensity modulation, like in traditional radio-over-fiber;
- on the AS, direct detection of the optical signal, then de-aggregation by a DSP similar to the one used at the Central Office (CO), and antennas feeding of the resulting N_{ch} radio waveforms, after proper frequency up-conversion.

Another approach based on Time Division Multiplexing (TDM) has also been proposed [7], but we will focus on the FDM version only.

To the best of our knowledge, the FDM DSP-A approach has been mainly investigated for DS purposes only [6, 8, 9], *i.e.*, for information flows from the base-band units (BBUs), typically placed in COs, to the AS that delivers the radio signals to the mobile terminals, whereas little attention was placed in the upstream (US) direction [10, 11]. Moreover, literature in this area mostly presents experimental analysis, with little emphasis on the link optimization. This paper focuses on these two missing aspects and, in particular, it deals with an equalization optimization procedure that can be applied to both DS and US directions.

The quality of the optical DS link is evaluated in our paper focusing only on the Error Vector Magnitude (EVM)

Manuscript received August 31, 2017.

P. Torres-Ferrera and R. Gaudino are with Politecnico di Torino, 10129 Torino, Italy. pablo.torres@polito.it.

S. Straullu and S. Abrate are with Istituto Superiore Mario Boella, 10138 Torino, Italy. straullu@ismb.it.

parameter. We did not consider here the processing delay, since it was anyway already studied in [6], where it is shown that FDMA-based DSP aggregation can be implemented with delays that satisfy even the very stringent requirements that have been set, for instance, for CPRI. Moreover, we also did not consider the Alternate Channel Leakage Ratio (ACLR) parameter since, even though it is very important for this kind of system, it would require a further extensive study that cannot fit in the space limitation of this paper. Most of the transmission experiments carried out so far foresee the transmission of a set of radio signals that are generated by DSP platforms at the CO as "error-free" signals (EVM = 0%) and then sent over a fiber infrastructure. The optical link is terminated at the AS where the received signal should comply with the EVM values required by today LTE standards [12] and, in the near future, by the 5G requirements. To achieve the required performance, a set of DSP techniques and optimization procedures have been proposed and analyzed in some of our previous works using the DSP-A approach for the DS scenario [8, 9].

For what concerns the US direction, the problem is reverted with respect to DS, as schematically depicted in Fig. 1, in the sense that the signal to be transmitted over the fiber path is already corrupted by the radio propagation. In addition, mobile terminals are randomly distributed within the radio cell, and thus all electrical carriers reach the antenna, and then the electro-optical converters, with different EVM on a per-channel basis. Properly conditioning the aggregated signal then becomes the key aspect for dimensioning the optical link towards the BBU.

In this paper we analyze, for the first time to the best of our knowledge, the problem to be faced by the US link of an optical fronthauling network based on DSP-A, which is the aggregation of many radio signal characterized by different EVM. We propose an equalizing rule to be applied to the signal transporting all the different electrical carriers generated by the mobile terminals that optimizes the overall system performance and, in parallel, can also cope frequency-dependence on the optical link (in terms of either transfer function and/or noise). Moreover, we show that the proposed equalizer derived for the US direction could be easily adapted to work also for DS conditions, which will be treated as a special (and simpler) case of the general US problem. In the following, for the sake of completeness, we replicate some results reported in [9] to exemplify the equalization functionalities under the DS scenario. In addition, a novel EVM estimation technique performed using the DSP aggregation (or de-aggregation) block functionalities, which enables a realistic EVM measurement under real-time conditions, is also proposed and analyzed. The additional complexity of implementing this technique in a DSP-A architecture is almost marginal.

The paper is thus organized as follows: in Section II we develop the theory behind the proposed equalization algorithm, then in Section III the experimental setup is described. In Section IV we propose an EVM practical estimation technique, whereas in Section V and VI the results of the experimental campaign for the DS and US directions, respectively, are shown; finally, in Section VII we draw some conclusions.

II. Pre-emphasis equalization technique: general theoretical treatment

We assume that, at the transmitter side, a set of N_{ch} complex baseband digital OFDM waveforms s_i, $i \in [1, N_{ch}]$ (which today can represent LTE-A signals or, in the near future, 5G radio signals), are aggregated following the DSP-based approach described in [6]. The signal to be transparently transported over the optical link can thus be written as:

$$x_{FDM}(t) = \sum_{i=1}^{N_{ch}} x_{OFDM,i}(t) = \sum_{i=1}^{N_{ch}} \mathrm{Re}\left\{ s_i(t) \exp\left(j2\pi f_i t \right) \right\} \quad (1)$$

where $x_{OFDM,i}(t)$ represent the signals that results after RF-up conversion of the complex baseband signals s_i, and f_i are properly selected electrical frequencies to perform FDM aggregation. These OFDM signals exhibit, in general, different SNR values at the output of the fronthaul channel in both DS and US directions, which results in a non-uniform EVM distribution among channels. This channel dependent performance occurs because of the frequency-dependence on the optical link. In the US direction, additionally, the performance of the channels at the input of the fronthaul is already unbalanced due to wireless propagation. Since all the channels should outperform a given EVM target at the receiver side, the maximum Optical Path Loss (OPL) of the system, for a given transmitted power, becomes limited by the worst performing channel, whereas the rest of them would still have a performance margin to allow an OPL increasing. To compensate for this issue, the aggregated channels can be pre-emphasized in amplitude at the transmitter side in order to obtain approximately the same EVM at the receiver side and thus approximately the same Bit Error Rate (BER).

The proposed pre-emphasis technique consists on multiplying the amplitude of each s_i waveform by a properly selected real coefficient k_i, as shown in Fig. 2. After pre-emphasis, the $x_{FDM}(t)$ signal becomes:

$$x_{FDM}(t) = \sum_{i=1}^{N_{ch}} k_i x_{OFDM,i}(t) \quad (2)$$

The set of k-coefficients are globally optimized in order to minimize the maximum received EVM (which is equivalent to maximize the minimum received SNR), along the whole set of channels. An algorithm to carry out this optimization is developed here as follows.

Let us analyze the more general case, corresponding to the US direction, to generate the pre-emphasis algorithm. The DS direction can be considered a particular case of the US one, as discussed later. A simplified model of the US transmission is shown in Fig. 3, where we have considered equivalent noise contributions for both the wireless and

optical segments. All the systems are considered linear, therefore, the propagation of each OFDM channels is assumed to be, as a first approximation, independent, in the sense that we neglect in this analysis nonlinearly generated crosstalk among channels. According to this model, the *i*-th OFDM signal at the output of the fronthaul receiver and DSP de-aggregator, $\tilde{s}_i(t)$, can be written as:

$$\tilde{s}_i(t) = k_i\left(s_i(t) + n_i^W(t)\right) + n_i^F(t) \tag{3}$$

where $s_i(t)$ is the signal generated by the *i*-th mobile terminal, and $n_i^W(t)$ and $n_i^F(t)$ are noise signals that emulates the noise addition to $s_i(t)$ after transmission through the wireless and the optical fronthaul channels, respectively. These noise signals are modelled here as additive white Gaussian noise (AWGN), each encompassing the sum of all the individual contributions of the noise sources present in the wireless and optical fronthaul system, respectively. In the following, we omit the dependence on time. The SNR of the *i*-th OFDM channel at the output of the fronthaul, SNR_i^{out}, is thus equal to:

$$\mathrm{SNR}_i^{out} = \frac{k_i^2 P_{s,i}}{k_i^2 P_{n^W,i} + P_{n^F,i}} = \frac{1}{\dfrac{P_{n^W,i}}{P_{s,i}} + \dfrac{1}{k_i^2}\dfrac{P_{n^F,i}}{P_{s,i}}} \tag{4}$$

where $P_{s,i}$, $P_{n^W,i}$ and $P_{n^F,i}$ are the average power of s_i, n_i^W and n_i^F, respectively. After very simple mathematical passages, Eq. (4), can be expressed as:

$$\left(\mathrm{SNR}_i^{out}\right)^{-1} = \left(\mathrm{SNR}_i^{W}\right)^{-1} + \left(k_i^2 \cdot \mathrm{SNR}_i^{F}\right)^{-1} \tag{5}$$

where $\mathrm{SNR}_i^W = P_{s,i}/P_{n^W,i}$ and $\mathrm{SNR}_i^F = P_{s,i}/P_{n^F,i}$, are the "individual" SNR that would be present at the output of the wireless and the optical fronthaul channels, respectively, if they were single independent "blocks" with an input signal s_i. Since both the wireless and the optical fronthaul channels are here modeled as AWGN channels, the SNR and the root-mean-square EVM of the signal are thus related as $\mathrm{SNR}_i = 1/\left(\mathrm{EVM}_i\right)^2$ [13]. Using this relation, Eq. (5) can be rewritten in terms of EVM as follows:

$$\left(\mathrm{EVM}_i^{out}\right)^2 = \left(\mathrm{EVM}_i^{W}\right)^2 + \left(k_i^{-1} \cdot \mathrm{EVM}_i^{F}\right)^2 \tag{6}$$

$$\text{Then, } k_i = \sqrt{\frac{\left(\mathrm{EVM}_i^{F}\right)^2}{\left(\mathrm{EVM}_i^{out}\right)^2 - \left(\mathrm{EVM}_i^{W}\right)^2}} \tag{7}$$

This last expression indicates a useful way to compute the k_i coefficient for a given set of EVM_i^{out}, EVM_i^W and EVM_i^F values. The last two terms are the EVM of the *i*-th signal at the output of the wireless and the optical fronthaul channels, respectively, and they can be measured directly on the signals involved in the fronthauling system. The term EVM_i^F is the EVM that would be obtained at the output of the fronthaul segment if only the noiseless signal s_i was present at its input (without noise addition at the wireless channel) but, unfortunately, this term cannot be measured directly. We thus propose an easy, two-step procedure to solve the issue. In particular, for a given setup, a first transmission in which each k_i coefficient is equal to one is performed (no pre-emphasis situation) and each resulting EVM_i^{out}, named here $\mathrm{EVM}_i^{out,no-pre}$, is measured at the receiver side. Each EVM_i^F is then computed at the transmitter, following Eq. (7) with k_i =1, as follows:

$$\mathrm{EVM}_i^F = \sqrt{\left(\mathrm{EVM}_i^{out,no-pre}\right)^2 - \left(\mathrm{EVM}_i^{W}\right)^2} \tag{8}$$

This process solves the problem of practically evaluating EVM_i^F. We notice that it should be repeated every time the optical channels conditions change significantly.

As stated before, the objective of the pre-emphasis technique is to minimize the maximum EVM_i^{out}. It can be shown that this optimization problem is equivalent to enforce a uniform EVM per channel distribution, *i.e.,* enforcing EVM_i^{out} to be constant and equal to a given target value: $\mathrm{EVM}_i^{out} = \mathrm{EVM}_{\mathrm{target}}^{out}$, $\forall i = 1, 2, ..., N_{ch}$. By considering this condition, and substituting Eq. (8) into Eq. (7), the k_i coefficient is evaluated by means of the following expression:

$$k_i = \sqrt{\frac{\left(\mathrm{EVM}_i^{out,no-pre}\right)^2 - \left(\mathrm{EVM}_i^{W}\right)^2}{\left(\mathrm{EVM}_{\mathrm{target}}^{out}\right)^2 - \left(\mathrm{EVM}_i^{W}\right)^2}} \tag{9}$$

This is the main result of this section, since it completely solves the problem on how to evaluate the equalization k_i coefficient in an optimal and very practical way. Since $\mathrm{EVM}_i^{out,no-pre} \geq \mathrm{EVM}_i^W$, $\forall i \in N_{ch}$, then a lower bound to choose the $\mathrm{EVM}_{\mathrm{target}}^{out}$ is $\mathrm{EVM}_{\mathrm{target}}^{out} > \mathrm{EVM}_i^W$, $\forall i \in N_{ch}$, in order to compute a set of real-valued *k*-coefficients.

Given a set of EVM^W per channel at the input of the fronthaul, the corresponding set of $\mathrm{EVM}_i^{out,no-pre}$ per channel at its output when no pre-emphasis is applied depends only on the characteristics of the optical fronthaul. Then, from Eq. (9), the only parameter that can be chosen to evaluate the *k*-coefficients is the $\mathrm{EVM}_{\mathrm{target}}^{out}$. However, it is important to note that $\mathrm{EVM}_{\mathrm{target}}^{out}$ is not a completely free parameter that can be arbitrarily chosen. In fact, since after pre-emphasis the amplitude of the signal will change as a function of the computed *k*-coefficients, the choice of $\mathrm{EVM}_{\mathrm{target}}^{out}$ needs to be constrained in such a way that the

resulting peak-to-peak voltage (V_{pp}) of the signal $x_{FDM}(t)$ equals the optimum voltage range in which the optical modulator is driven. To better understand this point, we remember that in order to reduce the peak-to-average power ratio (PAPR), in all these kinds of FDM-aggregated systems, the signal $x_{FDM}(t)$ needs to be amplitude clipped with a properly optimized clipping ratio [9]. The actual $x_{FDM}(t)$ optimal peak-to-peak voltage at the input of the modulator is related to its variance σ^2_{FDM} before clipping as $V_{pp} = C_{clip} \cdot \sigma_{FDM}$ [9], where C_{clip} is a proper optimal clipping level parameter. Therefore, provided that the pre-emphasis technique is applied before clipping, in order to force the same V_{pp} before and after the pre-emphasis block, the $\mathrm{EVM}^{out}_{\mathrm{target}}$ value is actually constrained to maintain after pre-emphasis the same variance of the signal $x_{FDM}(t)$ that was present before the technique is applied. We verified by extensive simulations and experiments that this heuristic rule is actually the one leading to optimal results. Considering that the individual OFDM waveforms can be modeled (with very good level of approximation) as independent Gaussian random variables, the variance of $x_{FDM}(t)$ before pre-emphasis can be evaluated as $\sigma^2_{FDM} = \sum_{i=1}^{N_{ch}} \sigma_i^2$, where σ_i^2 is the variance of s_i. If the variance of all OFDM signals is assumed to be the same, *i.e.*, $\sigma_i^2 = \sigma^2_{OFDM}$, $\forall i \in N_{ch}$ (a very reasonable assumption in the fronthauling scenario, since all OFDM channels can be properly normalized in DSP), then the variance of $x_{FDM}(t)$ can be computed as $\sigma^2_{FDM}(t) = N_{ch} \cdot \sigma^2_{OFDM}$. Once the pre-emphasis technique is applied, the variance of the signal $x_{FDM}(t)$ before clipping (see Eq. (2)) becomes:

$$\sigma^2_{FDM} = \sum_{i=1}^{N_{ch}} k_i^2 \sigma_i^2 = \sigma^2_{OFDM} \sum_{i=1}^{N_{ch}} k_i^2 \tag{10}$$

Therefore, in order to preserve the variance of $x_{FDM}(t)$ after pre-emphasis to the same value as for the no pre-emphasis case, the following condition should be satisfied:

$$\sum_{i=1}^{N_{ch}} k_i^2 = N_{ch} \tag{11}$$

Let us define a G_{US} function as follows:

$$G_{US} = \frac{1}{N_{ch}} \sum_{i=1}^{N_{ch}} k_i^2 \tag{12}$$

By substituting Eq. (9) into Eq. (12), we get G_{US} as a function of $\mathrm{EVM}^{out}_{\mathrm{target}}$, as following:

$$G_{US}(\mathrm{EVM}^{out}_{\mathrm{target}}) = \frac{1}{N_{ch}} \sum_{i=1}^{N_{ch}} \left(\frac{\left(\mathrm{EVM}_i^{out,no-pre}\right)^2 - \left(\mathrm{EVM}_i^{W}\right)^2}{\left(\mathrm{EVM}^{out}_{\mathrm{target}}\right)^2 - \left(\mathrm{EVM}_i^{W}\right)^2} \right) \tag{13}$$

From Equations (11) – (13) it is straightforward to see that the choice of $\mathrm{EVM}^{out}_{\mathrm{target}}$ is then constrained to satisfy the condition $G_{US} = 1$, where G_{US} is the constraint function in the optimization process to minimize the maximum EVM of the received set of EVM per channel values. Therefore, the $\mathrm{EVM}^{out}_{\mathrm{target}}$ that solves the condition $G_{US} = 1$ in Eq. (13) represents the minimum (*i.e.,* optimum) EVM value that can be achieved by all the OFDM channels.

Equations (9) and (13) are, in our opinion, a very important result in the channel performance equalization procedure for DSP-A fronthauling system and, to the best of our knowledge, this equalization algorithm was never proposed in literature before. Moreover, the additional DSP complexity of the proposed pre-emphasis technique is marginal since, as also shown in Fig. 3, it requires only N_{ch} real multiplication blocks in the fast part of the DSP flows, whereas the update of the k coefficients could be implemented off-line by a slow processing, considering that the optical channel is almost static. The practical application of these equations will be explained in Section VI on experimental upstream transmission demonstration.

Let us now adapt the equalization algorithm to the DS direction. Whereas in the US case the OFDM generator block, shown in Fig. 3, emulates the mobile terminals, in the DS scenario this block emulates the BBUs, followed by the optical fronthaul channel. This situation is equivalent to consider an US scenario in which a noiseless wireless channel is placed in between the BBUs and the optical fronthaul. Therefore, all the previous analysis carried out for the US case are still valid for the DS one if considering that $\mathrm{EVM}_i^{W} = 0$. Consequently, Eq. (9) and Eq. (13) largely simplify to:

$$k_i = \frac{\mathrm{EVM}_i^{out,no-pre}}{\mathrm{EVM}^{out}_{\mathrm{target}}} \tag{14}$$

$$\text{and, } G_{DS}(\mathrm{EVM}^{out}_{\mathrm{target}}) = \frac{1}{N_{ch}} \sum_{i=1}^{N_{ch}} \left(\frac{\mathrm{EVM}_i^{out,no-pre}}{\mathrm{EVM}^{out}_{\mathrm{target}}} \right)^2 \tag{15}$$

The functionality of the proposed pre-emphasis technique for the DS direction is experimentally evaluated in Section V, replicating some results of our previous work reported in [9], for the sake of completeness.

III. Experimental Setup

The experimental setup for the proposed DSP-A fronthauling system is shown in Fig. 4, where either the DS or US directions of a fronthauling architecture can be emulated just by making different assumptions on the characteristic of the input signals, as detailed below. At the transmitter side, N_{ch} = 96 baseband radio waveforms (generated in Matlab® to satisfy LTE-A standard

requirements) are aggregated to form the $x_{FDM}(t)$ signal following the DSP-assisted approach proposed in [6], using 96 FFT blocks of size N = 16 and an inverse FFT block of size M = 4096. Each radio waveform is an OFDM signal using 64-QAM as digital modulation format and generated with a 30.72 MHz sampling rate, according to the specification of a 20 MHz LTE-A signal. The resulting channel spacing between the central frequencies of two adjacent radio waveforms is exactly set at 30.72 MHz, so that the total electrical spectrum is approximately equal to 3 GHz. This choice allows a very straightforward DSP aggregation procedure. The $x_{FDM}(t)$ signal is stored in an Arbitrary Waveform Generator (AWG), characterized by an analog bandwidth of 6 GHz, a vertical resolution of 10 bits and a sampling rate of 12 GS/s. To emulate the US transmission case, AWGN is added to each off-line generated OFDM signal before DSP-A FDM aggregation. This noise addition emulates, in our experimental setup, the propagation of the signals through the wireless channel. The variance of the AWGN added to each OFDM channel is properly set to achieve a particular EVM value at the input of the fronthaul, which is, in general, different among channels, as detailed in Section VI. In the DS direction, the OFDM signals are generated as error-free without any noise addition before entering the fronthaul system.

A Mach-Zehnder Modulator (MZM), driven by the $x_{FDM}(t)$ signal is used to modulate the continuous wave (CW) carrier generated by the laser source. The MZM is biased at its quadrature point [8]. The optical signal at the output of the modulator is amplified using an erbium doped fiber amplifier (EDFA). The transmitted output optical power (P_F) is set to +9 dBm. The transmitter output signal is launched into 25 km of SMF followed by a variable optical attenuator (VOA) for spanning different values of OPL. Then, an avalanche photodiode (APD) directly detects the signal. We used an APD that is today typical for next-generation Passive Optical Network architecture (such as XGS-PON or NG-PON2) that, due to their high sensitivity requirements, cannot use a standard PIN-based photodiode. It is followed by a transimpedance amplifier and a real-time oscilloscope (RTO) which performs analogue-to-digital conversion (ADC) and stores the resulting samples. The RTO is characterized by 16 GHz of analogue BW, 50 GS/s of sampling rate and 8 bits of vertical resolution. The EVM calculation is carried out in Matlab® by applying the de-aggregating, post-processing algorithm on the signals stored by the RTO and then demodulating each OFDM signal. An ideal synchronization scheme was performed based on a cross-correlation operation between the received signal and a pilot signal. The de-aggregation procedure is performed following the DSP-based approach using an FFT block of size M = 4096 and 96 inverse FFTs blocks of size N = 16. After applying single-tap frequency domain equalizers, the EVM per channel is obtained as the average over all the OFDM subcarriers.

IV. Spectral EVM Estimation

In order to measure the EVM of each OFDM channel, either at the input or output of the fronthaul, a full OFDM receiver per channel is needed. In our laboratory experiments this procedure was performed off-line in Matlab®, but in a real fronthaul implementation this would be exceedingly complex to be carried out in the AS. For this reason, a simpler approach in which each EVM_i value is estimated from spectrally measuring the corresponding SNR_i on every channel without passing from the EVM_i evaluation at the OFDM receivers is here proposed. In the proposed approach, named here "spectral EVM estimation", a direct SNR_i estimation is performed based on the parameters available in the DSP that implements channel aggregation/de-aggregation at the transmitter/receiver. In particular, at the receiver, each SNR_i is obtained by averaging the values of several frames at the output of the M-points FFT that has to be performed for channel de-aggregation, which is thus used as a form of "embedded" electrical spectrum analyzer, without requiring any further DSP complexity. Let us name the received signal after analogue to digital conversion and synchronization as $\tilde{x}_{FDM}[n]$. This signal is serial to parallel converted to form the parallel signal $\tilde{x}_P$ as following:

$$\tilde{x}_P = \begin{bmatrix} \tilde{x}_P[0,0] & \tilde{x}_P[0,1] & \tilde{x}_P[0,2] & \dots \\ \tilde{x}_P[1,0] & \tilde{x}_P[1,1] & \tilde{x}_P[1,2] & \dots \\ \dots & \dots & \dots & \dots \\ \tilde{x}_P[\text{M-}1,0] & \tilde{x}_P[\text{M-}1,1] & \tilde{x}_P[\text{M-}1,2] & \dots \end{bmatrix}$$

$$\tilde{x}_P[i,\, j] = \tilde{x}_{FDM}[i + j\text{M}]$$

After the M-points FFT block, the parallel signal $\tilde{x}_P$ becomes the parallel complex signal $\tilde{\text{X}}_P$:

$$\tilde{\text{X}}_P = \begin{bmatrix} \tilde{\text{X}}_P[0,0] & \tilde{\text{X}}_P[0,1] & \tilde{\text{X}}_P[0,2] & \dots \\ \tilde{\text{X}}_P[1,0] & \tilde{\text{X}}_P[1,1] & \tilde{\text{X}}_P[1,2] & \dots \\ \dots & \dots & \dots & \dots \\ \tilde{\text{X}}_P[\text{M-}1,0] & \tilde{\text{X}}_P[\text{M-}1,1] & \tilde{\text{X}}_P[\text{M-}1,2] & \dots \end{bmatrix} = \begin{bmatrix} \tilde{\text{X}}_{Pt}[0] \\ \tilde{\text{X}}_{Pt}[1] \\ \dots \\ \tilde{\text{X}}_{Pt}[\text{M-}1] \end{bmatrix}$$

Let us now define the signal $\tilde{\text{X}}_{FDM}$ as follows:

$$\tilde{\text{X}}_{FDM}[m] = \tilde{\text{X}}_{FDM}\left[-M/2\right], \dots, \tilde{\text{X}}_{FDM}[0], \dots, \tilde{\text{X}}_{FDM}\left[M/2 - 1\right]$$

$$\tilde{\text{X}}_{FDM}[i] = mean_L\left(\left|\tilde{\text{X}}_{Pt}\left[i + M/2\right]\right|^2\right) = \frac{1}{L}\sum_{j=0}^{L-1}\left|\tilde{\text{X}}_P\left[i + M/2, \text{j}\right]\right|^2$$

where $mean_L(\cdot)$ indicates averaging over L number of frames, and $|\cdot|^2$ indicates modulus squared operation. The digital signal $\tilde{\text{X}}_{FDM}$ approximates the power spectrum of the signal $\tilde{x}_{FDM}[n]$ (the approximation improves as M and L increases). After a proper channel allocation, a particular set of N points of the signal $\tilde{\text{X}}_{FDM}$ corresponds to an estimation of the spectrum of each LTE channel. From these N points, signal and noise power levels can be estimated to compute the SNR of each channel, and

therefore the EVM. This procedure is depicted in Fig. 5: the spectrum shown in the inset is simply the average modulus squared of the FFT output values, so that the SNR_i values can be estimated as the ratio between the average of seven signal points and the average of two "noise-floor" points (one at the left and one at the right side of each useful signal), as indicated in the zoom inset of Fig. 5. At the transmitter side, the same procedure can be performed to estimate the EVM of the channels at the input of the fronthaul, by using the outputs of the N_{ch} N-points FFTs of the DSP-assisted aggregator.

Unfortunately, by testing the proposed spectral EVM estimation method, we found a significant disagreement between the spectrally estimated and the actual EVM_i values measured using OFDM receivers. We thus tried to turn off some channels and repeat the SNR measurements. The corresponding power spectrum at the output of the de-aggregator's FFT is plotted in Fig. 6 for one of the experimental cases that will be presented in the following section. A mismatch between the noise levels measured when a channel is turned on and off is clearly evident. As depicted in Fig. 6, the actual noise level of the channels is hidden by the equivalent cross-talk generated by the finite spectral resolution of the FFT-based spectral estimation. This noise level mismatch is reflected in the referred EVM disagreement between the two EVM measurement techniques. To overcome this limitation, one channel at a time can be turned off in a proper initial "bootstrap" phase of the optical fronthauling system, so the corresponding actual noise level of that channel can be measured and stored. This operation should be performed periodically before sending the data. The optical fronthaul system is assumed to be static under that period. Once having the complete noise per channel vector stored, the SNR can be estimated by means of the actual power of the signal per channel (measured at real-time) and its corresponding noise value (stored). If the fronthaul setup changes, the procedure to measure and store the corresponding noise per channel vector must be repeated.

Figure 7 shows EVM per channel graphs for three experimental tests (setting different OPLs) in which the EVM values obtained by using the spectral estimation technique and the ones measured using full OFDM receivers are compared. It could be observed that the difference between the results obtained using the two procedures is very small, demonstrating the validity of the proposed spectral estimation proposal.

V. Downstream results

The ETSI standard requires EVM ≤ 8% for LTE-A 64-QAM signals at the transmitter antenna [12]. Due to the frequency response of the full opto-electronics used in our experiments, the received 96 channels have different amplitudes over the used 3 GHz band and the noise level is not flat. In our experiments, this is mostly due to the used DAC and ADC, whose amplitude response and effective number of bits is getting worse for increasing frequency. The frequency dependence would anyway be present in any optoelectronic system, particularly for the very high available bandwidth that will be required for future fronthauling solutions. As a consequence, we would always have significantly different EVMs among the received radio channels. Therefore, the transmitted amplitudes in the DSP domain were equalized using the approach described in Section II. The results are shown in Fig. 8 for two different OPL values: 25 and 29 dB. In both cases, the maximum received EVM outperforms the EVM target, in the former without using any pre-emphasis technique, whereas it is necessary in the latter case. The black curve (with squares) reports the received EVM without any amplitude pre-emphasis equalization, *i.e.,* $\mathrm{EVM}_i^{out,no-pre}$ in Eq. (14) and Eq. (15), showing an unacceptable variation among channels. For instance, a variation from EVM = 6% at lower frequencies to 11% at higher frequencies is shown in Fig. 8.b. The pre-emphasis coefficients (k_i) to equalize the received SNR, and thus the EVM, are evaluated using Eq. (14), where the $\mathrm{EVM}_{\mathrm{target}}^{out}$ value is computed using Eq. (15) by fulfilling the condition G_{DS} = 1. The blue curve (with circles) reports the EVM_i^{out} when the amplitude pre-emphasis equalization takes place. In both OPL cases, the functionality of the pre-emphasis technique is demonstrated, reducing the maximum EVM value from 8.1% and 11.5% to 6% and 7.5% for OPL = 25 and 29 dB, respectively. This example largely shows the system gain that can be obtained using our procedure. As another positive side effect, it can also be observed the flattening of the EVM per channel distribution.

The EVM values presented in the blue (with circles) curve of Fig. 8 were measured on all channels at the output of a full OFDM receiver for each of the 96 channels. As discussed in Section IV, this operation would likely be very complex in the AS of a fronthauling architecture. For this reason, EVM results using the proposed simpler spectral estimation approach, described in Section IV, are also presented with the red curves (with triangles) in Fig. 8. As expected, no significant degradation between the blue and red curves can be observed. Moreover, in all cases the maximum EVM is maintained below the 8% target. Since both approaches deliver similar results but the EVM measurement aided by OFDM receivers is simpler and faster when an off-line DSP approach is used, this alternative method will be used in the results reported in the rest of this document. However, to the best of our knowledge, the spectral EVM estimation technique proposed and demonstrated here is a novel and useful contribution for real-time DSP implementations that enables the possibility of using equalization and compensation techniques that require a fast channel performance estimation, as the pre-emphasis compensation algorithms proposed and used in this work.

VI. Upstream Results

In this section, an analysis of the upstream link in optical fronthauling networks based on DSP-assisted channel aggregation is reported. The effect of both wireless and optical fiber transmission on the EVM is taken into account.

Before proceeding, we would like to point out that current LTE standard specify the required physical layer

performance by means of: i) a target EVM at the transmitter antenna: this is what we have directly used in the previous section on DS; ii) a packet loss rate at the final receiver (*i.e.*, after the final OFDM receiver in the BBU), which is directly related to the overall BER. Indirectly, this also means that the EVM at the final receiver should satisfy some proper EVM constraint (which is anyway not indicated in the LTE standards). For simplicity, we thus perform EVM consideration also in this case.

Considering different distributions of the mobile terminals within a radio cell, the proposed pre-emphasis equalizer (presented in Section II) is applied to the signal transporting all the already noisy electrical carriers generated by the mobile terminals, and its functionality is experimentally tested. Since we did not have access to a real radio distribution system on so many different radio channels, we reproduced in our laboratory some test conditions in terms of the statistical distribution of the EVM^{W} of the signals reaching the antenna from the mobile terminals. In particular, we tested: a deterministic non-uniform distribution (sinusoidal), a random distribution and a uniform distribution. The random distribution was Gaussian. The sequences loaded in the AWG were thus programmed in order to force the distribution of EVM^{W} and the related pre-emphasis equalization algorithm explained in Section II.

Purpose of the experimental campaign is to receive, at the BBU site, all the different mobile carriers outperforming a certain EVM^{out} target. In particular, all experiments were performed considering an EVM target of 8%. According to the LTE standard the EVM target in the US direction after the full transmission system can be much worse than 8% (extremely strong FEC codes are used on the radio channels, so that the actually received EVM can actually be very high). Purpose of this section is mainly to demonstrate the functionality of the pre-emphasis equalization under the US conditions for a given arbitrary EVM target. Therefore, the EVM = 8% was just set as an indicative value to maintain the same target as in the DS direction, but the qualitative results would be maintained also for higher target EVM. In the following, the results of the experimental campaign are reported and discussed. The OPL was set to 20 dB, unless otherwise stated. This OPL value was chosen in order to have a wide margin to degrade the performance of the channels at the input of the fronthaul and still outperform the chosen received EVM target, and thus be able to demonstrate the functionality of the pre-emphasis technique even under stressed conditions.

A deterministic EVM^{W} per channel distribution at the input of the fronthaul was analyzed as a first approach. Although deterministic distribution scenarios are unrealistic in real-world US fronthaul implementation, they are useful for testing purposes. In a first test case, a sinusoidal distribution (chosen arbitrarily), over two full periods, ranging from 2% to 7% was imposed to the EVM^{W}, as plotted in black with squares in Fig. 9.a. This EVM^{W} distribution was set to obtain one of its peaks at the highest frequency channel, which is the most affected by the low-pass response of the transmission system. This guarantees analyzing the worst-case scenario. At the output of the fronthaul, an EVM^{out} distribution, plotted in blue with circles in Fig. 9.a, with variations from 4% to unacceptable values of up to 9.5% is obtained when pre-emphasis equalization is not applied ($\text{EVM}^{out,no\text{-}pre}$ situation). The measured EVM^{W} and $\text{EVM}^{out,no\text{-}pre}$ per channel values were used to compute the constraint function G_{US} as a function of $\text{EVM}^{out}_{\text{target}}$ (plotted in Fig. 9.b) using Eq. (13). The $\text{EVM}^{out}_{\text{target}}$ value that fulfills the constraint G_{US} = 1, is 7.55%. Following Eq. (9), different sets of pre-emphasis coefficients k_i are evaluated considering different $\text{EVM}^{out}_{\text{target}}$ values, including the one that fulfills the constraint G_{US} = 1. Figure 9.c shows the resulting EVM^{out} per channel obtained after pre-emphasizing the channels at the transmitter side using different $\text{EVM}^{out}_{\text{target}}$ values. It is interesting to note that the best performing EVM^{out} per channel curve among the analyzed ones, is obtained using the $\text{EVM}^{out}_{\text{target}}$ = 7.55% value. For lower and higher $\text{EVM}^{out}_{\text{target}}$ values, the corresponding EVM^{out} per channel curves are less flat and the maximum EVM^{out} is in all cases higher than the maximum one in which the G_{US} = 1 condition is satisfied. This, in turn, shows, for some illustrative examples, a right optimization process using the analytically derived constraint discussed in Section II. Moreover, the $\text{EVM}^{out}_{\text{target}}$ = 7.55% value, is approximately achieved by all channels. Therefore, these results corroborate that, by fixing the constraint G_{US} = 1, the maximum possible "flat EVM" at the output of the fronthaul can be found. The equalized results reported in the rest of this section were obtained using the corresponding optimum $\text{EVM}^{out}_{\text{target}}$.

The results obtained when the pre-emphasis technique is applied ($\text{EVM}^{out}_{\text{target}}$ = 7.55%) are replicated in red with triangles in Fig. 9.a. It is evident that the EVM^{out} per channel distribution now becomes more uniform, with all channels exhibiting an EVM below 8%. The functionality of the proposed pre-emphasis technique is clear in this case. It is worth to notice that when pre-emphasis is applied, the channels with the worst SNR (maximum EVM) at the input of the fronthaul are received at its output with a very small SNR (EVM) penalty. An almost transparent transmission through the fronthaul is experienced by these channels since their power is enhanced to compensate for their lower SNR. This is performed at the expense of a strong degradation of the SNR (and EVM) of the best performing channels at the input of the fronthaul, due to a reduction of the power of these channels. For instance, channels 24 and 72 change their EVM from EVM^{W} = 2% at the input to EVM^{out} ~7% and 7.5% at the output, whereas before applying the pre-emphasis the EVM degradation was less sharp, obtaining an EVM^{out} of around 4% and 5.4%, respectively. Then, the pre-emphasis is exploited to compensate for the optical segment frequency response and, at the same time, to balance the LTE channels performance.

Two more cases in which an EVM^{W} sinusoidal distribution is considered, under two more demanding scenarios, are depicted in Fig. 10. In the first case (Fig.

10.a), the maximum EVM^W is increased to 7.5% maintaining the minimum equal to 2%. In the second case (shown in Fig. 10.b) the minimum EVM^W is increased to 4% whereas keeping the maximum to 7%. Although the EVM^W conditions were stressed, when pre-emphasis equalization is applied, the EVM^{out} target is still accomplished in both cases. Note that, in the case depicted in Fig. 10.a, the transmission through the fronthaul experienced by the worst performing channels at the input of the fronthaul, is completely transparent. For this same case, an $EVM^{out}_{target} = 8.06\%$ for $G_{US} = 1$ is computed, which exactly corresponds to the maximum EVM^{out} obtained value when pre-emphasis is applied.

In order to test a more general situation, a random EVM^W distribution varying from 2% to 7.5% was enforced and the performance of the system was analyzed under these input conditions. Figure 11.a presents the EVM^W (in black with squares) and the EVM^{out} without pre-emphasis (in blue with circles) per channel distributions corresponding to the random case. It is observed that several channels have an EVM^{out} higher than the chosen target. Once the pre-emphasis technique is applied, the resulting EVM^{out} per channel distribution, shown in red with triangles in Fig. 11.b, is flatten. All the channels outperform the EVM target. The functionality of the pre-emphasis equalization technique under a more general situation is then demonstrated.

Another random distribution situation, whose results are shown in Fig. 12.a, was tested. An EVM^W distribution with reduced variations from 4% to 6% was defined. However, this time the OPL was increased to 25 dB. By comparing the blue curve with circles and the red curve with squares, a much flatter EVM^{out} distribution is observed when the pre-emphasis technique is applied, as expected. Again, all the channels are below the chosen EVM target.

Finally, a uniform EVM^W distribution was analyzed. The resulting EVM^{out} values with and without applying the pre-emphasis technique are shown in Fig. 12.b. In a real mobile network scenario, the EVM of the signals reaching the antenna from the mobile terminals (EVM^W) is far from being uniformly distributed over frequency. Nevertheless, we report this case because it represents the worst-case scenario for the upstream transmission because there is no SNR margin between channels, and all channels worsen after optical propagation. In this case, the pre-emphasis is mainly needed to compensate for the optical link frequency response, as in the downstream case. However, it is important to remark that the evaluation of the k_i coefficients is still different between this upstream uniform condition (in which $EVM^W_i = k_w$, being k_w a non-zero constant value) and the downstream one (in which $EVM^W_i = 0$) (compare Eq. (9) and Eq. (14)).

From this worst case scenario, it is shown that an $EVM \leq 8\%$ at the BBUs can be achieved after up to 20 dB of OPL for all 96 LTE channels, provided that a maximum EVM^W as high as 6% is considered (irrespective of the EVM^W per channel distribution) and pre-emphasis is employed. If the maximum input EVM^W or the EVM^{out} target change, the achievable OPL also changes. Therefore, since the maximum OPL value for the US direction can be different from that for the DS one, it is very important to dimension both directions of a link for a proper operation of the full system.

To conclude this section, it should be clarified that all our experiments were performed assuming a static performance of the LTE channels during the pre-emphasis procedure. In practice, the performance of these wireless signals could be highly dynamic. To verify the assumed static condition in a real-time scenario, the performance variation of the radio signals should be slower than the time required to: measure the EVM of the channels at the receiver, send back this information to the transmitter and adapt the *k*-coefficients of the pre-emphasis block. We should also point out that although the proposed pre-emphasis technique was demonstrated to work well under different scenarios for the DS and US cases, the EVM^{out} distribution is not completely flat in any of the analyzed situations. This slight deviation from an ideal flat case results from the difference between the assumed conditions to derive the equalization algorithm (see Section II) and the real conditions of the experiments. However, since this deviation is small in all cases, we could then consider our assumptions to be accurate enough.

VII. Conclusions

An original pre-emphasis technique focus on equalizing the received SNR, thus minimizing the maximum EVM per channel at the output of the fronthaul, was developed in this work for both downstream and upstream directions. In our further work, we will also investigate other important parameters for this kind of links, such as the ACLR.

The developed algorithm takes into account the EVM per channel values at the input of the fronthaul, called here EVM^W, which in the upstream case are different to zero and non-uniform among channels. The pre-emphasis technique was tested for different EVM^W distributions at the input of the fronthaul and its ability to equalize the EVM of all the channels at the output of the fronthaul was experimentally demonstrated for all the analyzed cases, including downstream just adapting the equalizer by considering an $EVM^W = 0$ condition for all channels.

The maximum OPL value for the upstream direction can be different from that for the downstream. Therefore, the importance of dimensioning and optimize not only the downstream but the upstream direction of a link for proper operation of the full system, was demonstrated.

ACKNOWLEDGMENT

This work was supported by CISCO under an SVCF grant titled “5G-PON”. The work was also partially supported by the POLITO PhotoNext center (www.photonext.polito.it). P. Torres-Ferrera also acknowledges the support of CONACyT and DGAPA – UNAM through PAPIIT grant IN103416.

REFERENCES

[1] A. Pizzinat, P. Chanclou, F. Saliou and T. Diallo, "Things You Should Know About Fronthaul," *Journal of Lightwave Technology*, vol. 33, no. 5, pp. 1077-1083, 2015.

[2] X. Liu and F. Effenberger, "Emerging optical access network technologies for 5G wireless," *Journal of Optical Communications and Networking*, vol. 8, no. 12, pp. B70-B79, 2016.

[3] J. Wang *et al.*, "Digital mobile fronthaul based on delta-sigma modulation for 32 LTE carrier aggregation and FBMC signals," *Journal of Optical Communications and Networking*, vol. 9, no. 2, pp. A233-A244, 2017.

[4] T. Pfeiffer, “Next generation mobile fronthaul and midhaul architectures [Invited],” *Journal of Optical Communications and Networking*, vol. 7, no. 11, pp. B28-B45, 2015.

[5] CPRI, "Specification V6.1, Common Public Radio Interface (CPRI) Interface Specification," 2014.

[6] X. Liu, H. Zeng, N. Chand and F. Effenberger, "Efficient Mobile Fronthaul via DSP-Based Channel Aggregation," *Journal of Lightwave Technology*, vol. 34, no. 6, pp. 1556-1564, 2015.

[7] X. Liu, H. Zeng, N. Chand and F. Effenberger, "CPRI-Compatible Efficient Mobile Fronthaul Transmission via Equalized TDMA Achieving 256 Gb/s CPRI-Equivalent Data Rate in a Single 10-GHz-Bandwidth IM-DD Channel," in *Optical Fiber Communication Conference (OFC),* Anaheim CA, United States, 2016, paper W1H.3.

[8] M. Befekadu, S. Straullu, S. Abrate and R. Gaudino, "Experimental Optimization of DSP-Aggregated Front-hauling Transmission for up to 4x96 LTE radio waveforms," in *42th European Conference and Exhibition on Optical Communication (ECOC)*, Dusseldorf, Germany, 2016.

[9] P. Torres-Ferrera, S. Straullu, S. Abrate and R. Gaudino, "Alternative Solutions for Fronthauling based on DSP-assisted Radio-over-Fiber," in *19th International Conference on Transparent Optical Networks (ICTON)*, Girona, Spain, 2017.

[10] M. Zhu, F. Li, F. Lu, J. Yu, C. Su, G. Gu and G.-K. Chang, “Wavelength Resource Sharing in Bidirectional Optical Mobile Fronthaul," in *Journal of Lightwave Technology*, vol. 33, no. 15, pp. 3182-3188, 2015.

[11] M. Xu, J.-H. Yan, J. Zhang, F. Lu, J. Wang, L. Cheng, D. Guidotti, and G.-K. Chang, "Bidirectional fiber-wireless access technology for 5G mobile spectral aggregation and cell densification," *Journal of Optical Communications and Networking*, vol. 8, no. 12, pp. B104-B110, 2016.

[12] ETSI, "Technical Specification 136 104 V12.6.0 (2015-02)," 2015.

[13] R. A. Shafik, M. S. Rahman and A. R. Islam, "On the Extended Relationships Among EVM, BER and SNR as Performance Metrics," in *International Conference on Electrical and Computer Engineering*, Dhaka, 2006.

Pablo Torres-Ferrera received the B.Eng., M.E.E. and Ph.D. degrees (with honors) in telecommunications in 2010, 2012 and 2017, respectively, from the National Autonomous University of Mexico (UNAM), Mexico City. He worked from 2012 to 2013 at Huawei Technologies Mexico in the implementation of OTN rings. As part of his PhD investigation work, he carried out research internships at Athens Information Technology (AIT), Athens, in 2014 and at Politecnico di Torino, Italy, in 2016. He is currently a Post-Doctoral Researcher at Politecnico di Torino, working in the field of optical access networks.

Stefano Straullu received the Graduate degree in telecommunications engineering from Politecnico di Torino, Turin, Italy, in 2005, with a thesis on the realization and testing of opto-electronic subsystems for packet-switched optical networks, completed in the Istituto Superiore Mario Boella (ISMB), Turin; and the Ph.D. degree in electronics and communications engineering from Politecnico di Torino, Turin, with a thesis on next-generation passive optical networks. In 2006, he joined the Integration Testing Team of Motorola Electronics S.p.A., Turin. Since May 2009, he has been a Researcher at the ISMB, Turin. He has published more than 60 journal and conference papers.

Silvio Abrate graduated in Telecommunications Engineering in 1999 at Politecnico di Torino, with a thesis about the distribution of satellite television over an in-building fiber infrastructure. Since 2001 he was with the Optical Networks Division of Alcatel S.p.A., in Vimercate (MI), working on SDH and WDM networks especially for Telecom Italia and South America's providers. Since February 2003 he is a senior researcher at Istituto Superiore Mario Boella, with the role of coordinator of the PHOtonic Technologies and Optical Networks Laboratory (PhotonLab) held by the institute in cooperation with Politecnico di Torino. Silvio Abrate is author or co-author of over 100 journal and conference papers, 3 book chapters and holds 4 U.S./European patents.

Roberto Gaudino Ph.D., is currently Associate Professor at Politecnico di Torino, Italy. His main research interests are in the long haul DWDM systems, fiber non-linearity, modelling of optical communication systems and in the experimental implementation of optical networks, with specific focus on access networks. In particular, in the last five years, he focused his activity on short-reach optical links using plastic optical fibers (POF) and on next-generation passive optical access networks (NG-PON2). Currently, he is working on ultra-high capacity systems for medium reach links. Previously, he worked extensively on fiber modelling, optical modulation formats, coherent optical detection, and on the experimental demonstration of packet switched optical networks. Prof. Gaudino spent one year in 1997 at the Georgia Institute of Technology, Atlanta, as a visiting researcher, where he worked in the realization of the MOSAIC optical network test-bed. From 1998, he was with the team that coordinated the development of the commercial optical system simulation software OptSim (acquired now by Synopsis). He is author or co-author of more than 200 papers in the field of Optical Coomunications. From 2009 to 2016 he was the coordinator of three projects in the area of optical access (EU FP6-IST STREP “POF-ALL” and "POF-PLUS" and EU FP7-ICT STREP project “FABULOUS”).

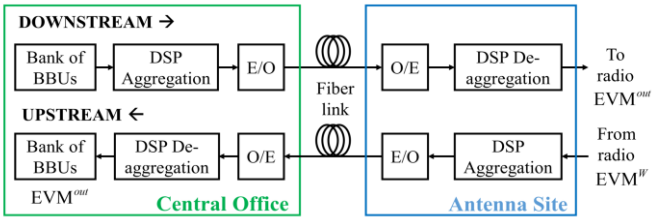

Fig. 1. Downstream and Upstream fronthauling path schemes (E/O: Electro-Optical converters, EVM^{W}: EVM due to radio path, EVM^{out}: EVM at the output of the fronthaul, O/E: Opto-Electrical converters).

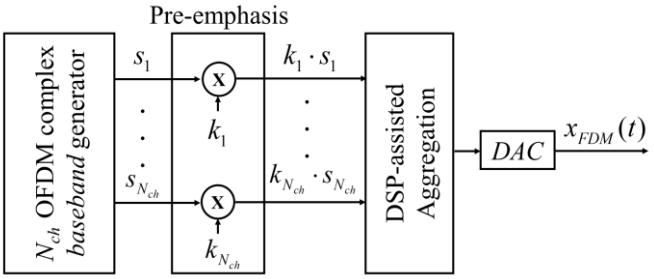

Fig. 2. Pre-emphasis technique diagram.

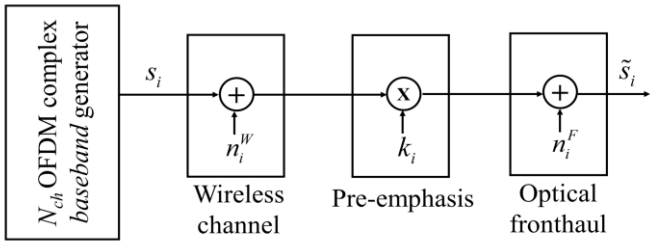

Fig. 3. Simplified model of the transmission in the upstream direction.

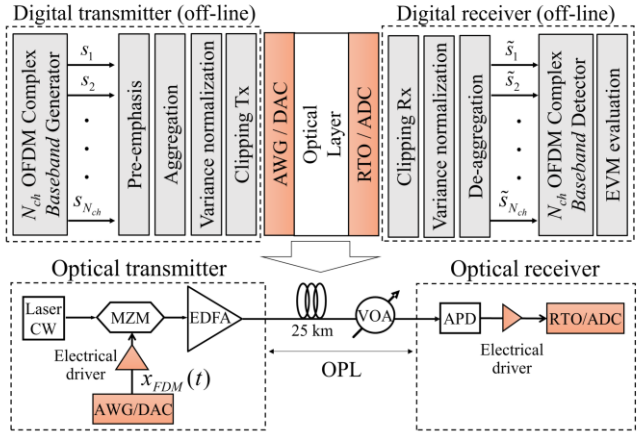

Fig.4. Experimental setup.

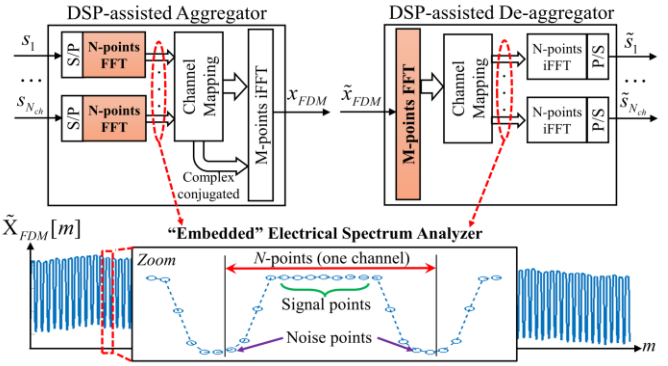

Fig. 5. Scheme of the SNR estimation technique aided by the electrical spectrum analyzer "embedded" into the DSP-assisted aggregator/de-aggregator blocks.

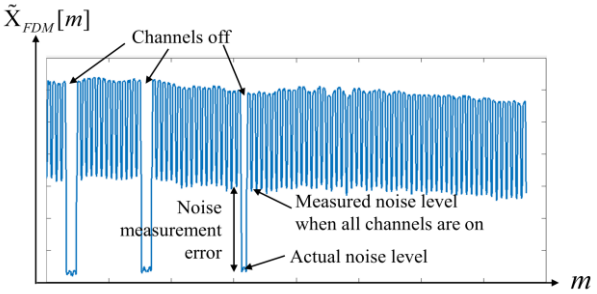

Fig. 6. Power spectrum obtained from the electrical spectrum analyzer "embedded" into the digital FDM de-aggregator when some channels are turned off.

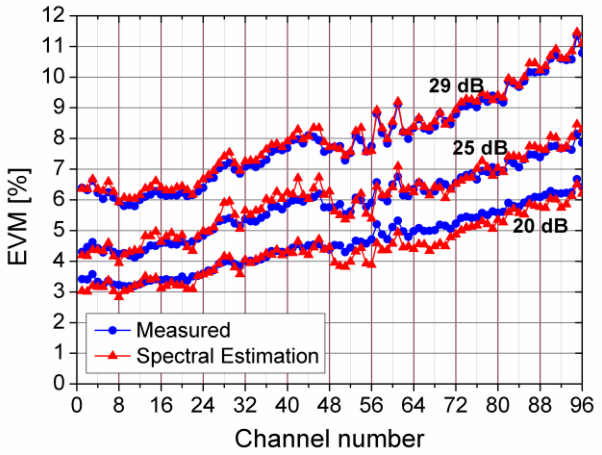

Fig. 7. EVM per channel graphs for three fronthauling conditions (OPL = 20, 25 and 29 dB). In blue with circles: measured using OFDM receivers. In red with triangles: obtained by spectral estimation.

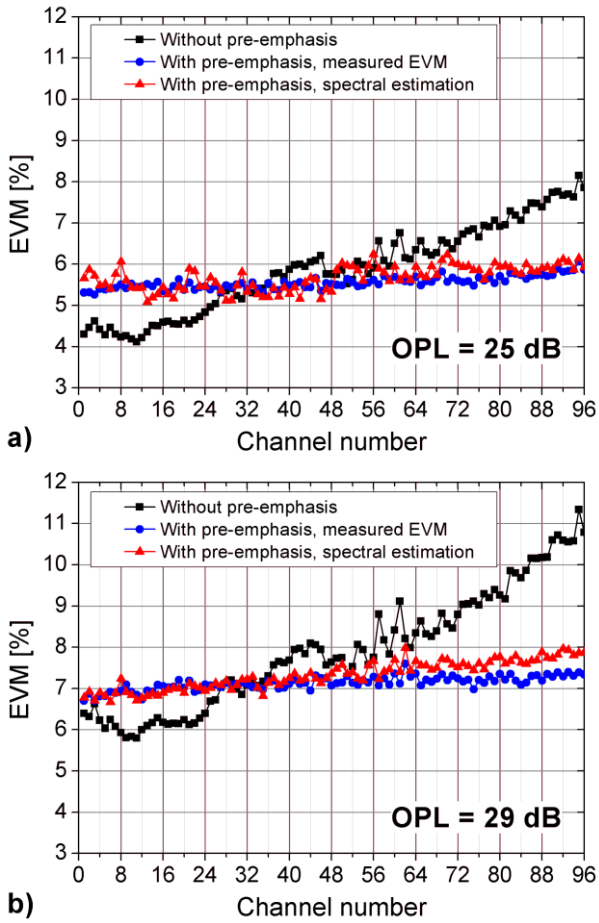

Fig. 8. EVM of the 96 OFDM channels at a) 25 dB and b) 29 dB of OPL before and after pre-emphasis equalization.

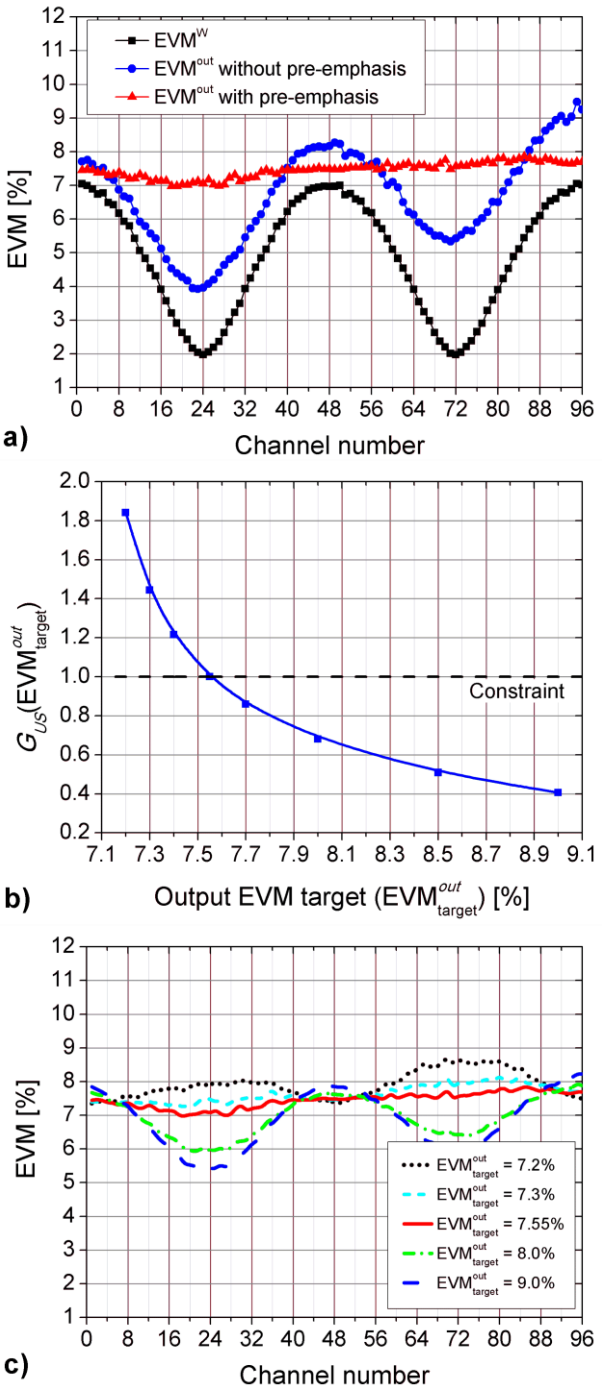

Fig. 9. a) Performance per channel for a sinusoidal EVM^{W} distribution: at the antenna site and at the BBU site after 20 dB of OPL with and without pre-emphasis; b) corresponding constraint function G_{US} versus EVM_{target}^{out}; and c) corresponding EVM^{out} per channel using pre-emphasis for different EVM_{target}^{out} values.

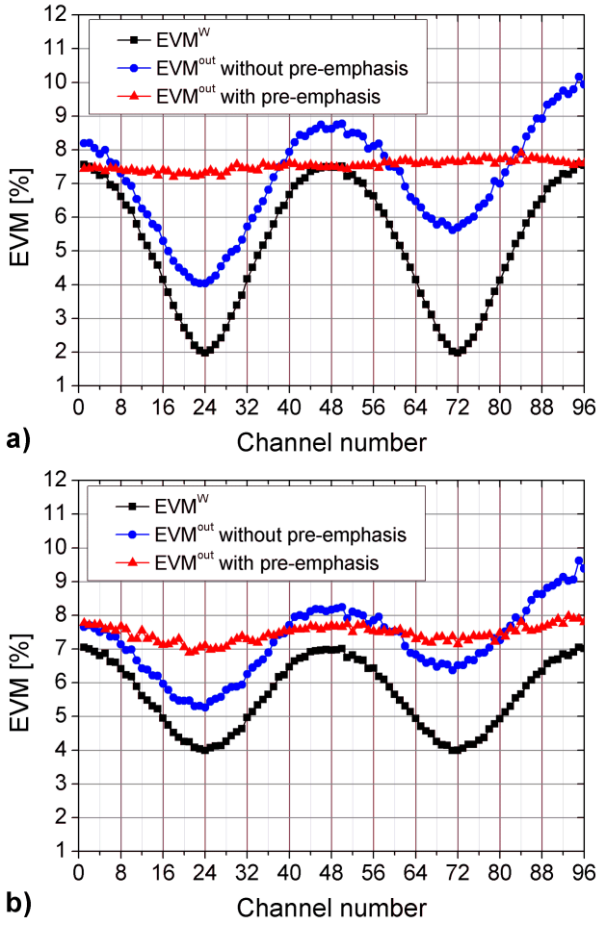

Fig. 10. Performance per channel for two sinusoidal EVM^W distributions, at the antenna site and at the BBU site after 20 dB of OPL with and without pre-emphasis.

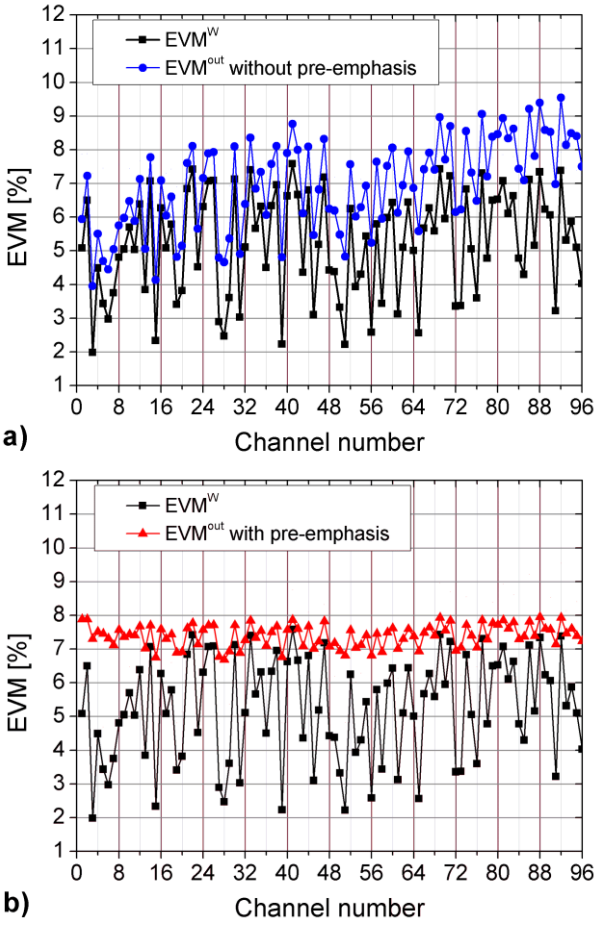

Fig. 11. Performance per channel for a random EVM^W distribution: a) at the antenna site and b) at the BBU site after 20 dB of OPL, with and without pre-emphasis.

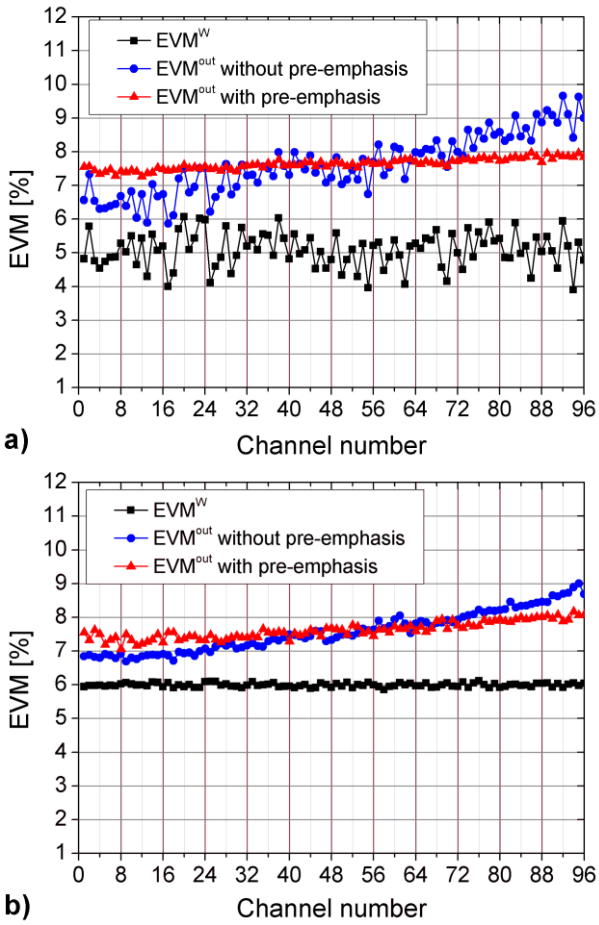

Fig. 12. Performance per channel for (a) a random and (b) a uniform, EVM^W distribution: at the antenna site and at the BBU site after 25 dB and 20 dB of OPL, respectively, with and without pre-emphasis.